Removal of heavy metal particles by LTJ, ANA, SVR, BEC and MER zeolites particles: A molecular dynamics simulation study

Mohsen Mehdipourghazi[1,*], Milad Mohammadi[2], Hamid Modares[3]

[1]*Faculty of Chemical, Petroleum, and Gas Engineering, Semnan University, 35131-19111, Semnan, Iran*

[2]*Department of Nanotechnology, New Sciences and Technologies Paradise, Semnan University, 35131-19111, Semnan, Iran*

[3]*Chemical Engineering Deapartment , Amirkabir University of Technology, Tehran, Iran*

HIGHLIGHTS

- Molecular dynamics simulation of heavy metal particles by zeolite particles was studied.

- The most of the particles had the highest affinity of ion exchanging with lead (II).

- The most of the particles had the lowest affinity of ion exchanging with copper (II).

- Maximum mean ion-exchange ratio belongs to ion with the highest ratio in single-ion system.

- Temperature variations had no significant effect on the mean ion-exchange ratios.

GRAPHICAL ABSTRACT
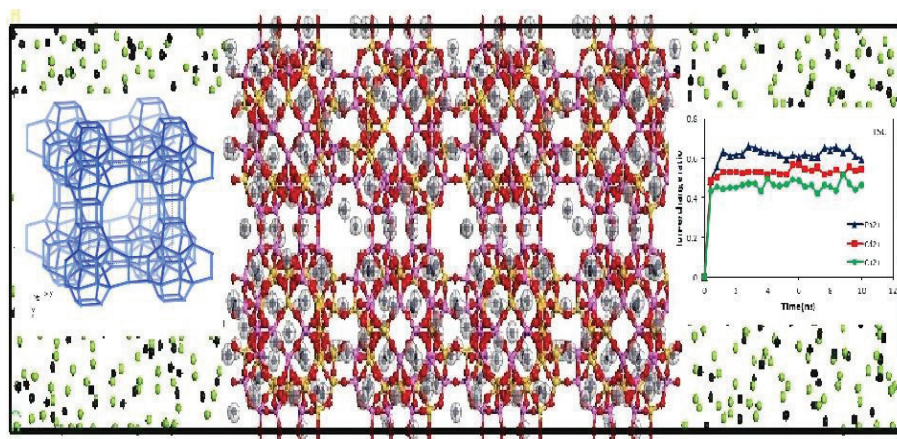
ABSTRACT

In present study, molecular dynamics simulation of Cadmium (II), Lead (II) and Copper (II) removal from aqueous electrolyte solutions using the ion-exchange process with the zeolite particles was done. The results showed that, most of the particles had the highest affinity of ion exchanging with Lead (II) and the lowest affinity with Copper (II). The calculated mean ion-exchange ratios showed that, except for the zeolites which their pore sizes are in the same range of heavy-metal ions' size, an inverse relationship exists between this ratios and pore size of the zeolites. Furthermore, the ion-exchanging of zeolites LTJ, ANA, SVR, BEC and MER with aqueous electrolyte mixtures containing equal amounts of Cadmium (II), Lead (II) and Copper (II) were simulated. The results demonstrated that in the competitive exchange of electrolyte mixtures, the maximum mean ion-exchange ratio belongs to the ion which has the highest ratio in the single-ion system. Moreover, ion-exchanging of zeolites LTJ, ANA, SVR, BEC and MER with an aqueous electrolyte solution containing Copper (II), in the temperature range of 300-345 K were simulated. The results revealed that, no significant change in the mean ion-exchange ratios were found as a result of temperature variations.

*Corresponding author. Tel.: +98 2333383922; fax: +98-2333654284

E-mail address:mohsenmehdipour@semnan.ac.ir (M. Mehdipourghazi).

1. Introduction

Several kinds of water pollutants are produced mainly by developed industrial activities. Many industries such as metal plating, mining, tanneries, dying, aerospace, battery, glass and ceramics release the hazardous heavy-metal pollutant ions such as Cu (II), Cd (II) and Pb (II). It is proved that these ions are tremendously toxic. Moreover, they can be extremely harmful to the environment, human health and all alive species [1,2]. As a consequence, it was absolutely vital to remove them from industrial waste water. Accordingly, numerous processes such as sorption, coagulation, sedimentation, ultrafiltration, reverse osmosis, electrodialysis, extraction, ion-exchange, and membrane processes have been developed [3].

Among the mentioned methods, ion-exchange process, because of their high technological feasibility and costing, is very attractive to many researchers and industries. Inorganic ion-exchangers such as zeolites, due to their distinguished properties such as high thermal stability and resistant to radiation are often preferred to the organic resins [4]. Zeolites are one of the ion-exchanging materials which their charge balancing cations can easily be substituted by cations in an electrolyte solution. Both natural and synthetic form of zeolites was used for removal of heavy-metal ions [5-19].

Pepe et al. used a mixture of two natural zeolites, including chabazite and phillipsite, for removal of Barium (II). Their investigation showed the high selectivity of Barium (II) in varied concentrations [5]. Ören et al. studied the pH and initial ion concentration effects on Zinc (II) removal with two natural zeolites. The process showed a strong dependence on pH and the removal capacity. This trend, firstly, increased by metal ion concentration and then became constant at higher concentrations [18].

Ahmed et al. investigated of four heavy-metal ion's removal by Na–Y zeolite under competitive and non-competitive conditions. Their results showed that under identical experimental conditions, Lead (II) ion removal was much greater than that of Cadmium (II). Moreover, the Na–Y zeolite exchange efficiency in the competitive condition for divalent heavy-metals was reported as Nickel< Copper< Cadmium<Lead [7]. Ismail et al. studied the removal of few metal ions by synthetic zeolite A. They showed that the effects of pH, ion concentration and amount of zeolite are significant but shaking time and reaction temperature is insignificant. Furthermore, they compared the activity of zeolite 4A with non-zeolite crystalline materials and amorphous synthesis products in removal of heavy-metal ions. Zeolite 4A, Because of larger pore size, provided more facile intra-particle diffusion for metal ions and had the higher IER (ion-exchange ratio) [6].

Molecular simulations have become a robust tool for studying the micro and nano scale processes. They can provide microscopic data, which are conducive to understand the processes in detail and subsequently can be used in rational design of materials. Molecular simulations have been used to investigation of important features of zeolites, including dynamics of cations distribution, hydrated and dehydrated structures, process rate, framework flexibility and small mobile species behavior in the zeolite pores [20-26].

Nalaparaju and co-workers studied molecular dynamic simulation in the single and triple ion-exchange of Lead (II), Cadmium (II), and Copper (II) with Na-ETS-10 titanosilicate zeolite membrane. They applied the implicit solvent method to decrease of the computational simulation time. Acceptable results obtained for lead (II) showed a strong affinity to the Na-ETS-10. Furthermore, the presence of Cadmium (II) and Copper (II) ions had no effect on the residence of Lead (II) in the membrane [4]. Ekhtiyari et al. investigated the effects of ion concentrations in and out of the LTA zeolites membrane, temperature, and membrane thickness on the silver-sodium ion-exchange dynamics [26].

In this work, the ion-exchange of several zeolites in aqueous solutions, containing heavy-metal ions of Lead (II), Cadmium (II) and Copper (II) are investigated by molecular dynamics simulations. This simulation helps to find out the effects of zeolite pore size and pore symmetry. The selected zeolites were: LTJ, ANA, SVR, MER, AFY, BEC, MEL, SGT, SAO, OBW, SBT, FAU, VFI and TSC. In addition, the process was simulated with zeolites of ANA, LTJ, BEC, MEL, and SVR in the temperature range of 300-345 K and in presence of the three ions to study of temperature and competitive condition effects.

2. Simulation methodology

The interactions were considered as the pair-wise additive between all atoms and ions. The dispersion interactions, attraction and repulsion, were expressed by the 12–6 Lennard-Jones (LJ) model by including the coulombic term for the long-range interactions, as given by the equation 1.

$$u_{ij}(r) = 4\varepsilon_{ij}\left[\left(\frac{\sigma_{ij}}{r_{ij}}\right)^{12} - \left(\frac{\sigma_{ij}}{r_{ij}}\right)^{6}\right] + \frac{q_i q_j}{4\pi\varepsilon_0\, r_{ij}\varepsilon_r} \quad (1)$$

Where r_{ij} is the inter-atomic distance, q_i and q_j are the atomic charge of i and j. Moreover, ε_{ij} and σ_{ij} are respectively the LJ cross interaction parameters which were evaluated by the Lorents–Berthelot mixing rules [27]. The permittivity of vacuum (ε^0) was 8.8542×10^{-12} $C^2\ N^{-1}\ m^{-2}$ [4,14].
The implicit solvent method was applied and water was treated as a continuum with dielectric constant $\varepsilon_r = 78$. This method has been used successfully in previous studies for removal of heavy-metal ions by ion-exchange process with zeolites which produced acceptable results in comparison with presence of water molecules [4,26]. The values of atomic charges q_i and q_j were used from the previous work of Ekhtiyari et al. [26]. The LJ interactions were evaluated with a spherical cut-off 12.5 Å and the long-range corrections were included. The Ewald sum with a thin-foil boundary condition was used to compute the Coulombic interactions. The ions were assumed as rigid bodies with the effective partial charges and the polarization effects were neglected. Also, the Cl⁻ ions were used as negative ions in the solution compartments. The parameters for all the atom types are summarized in Table1.

The zeolites' data were obtained from the Database of Zeolite Structures [30], and the Al/Si ratios were considered as unity. The simulation boxes were prepared according to the following steps:
1- To satisfy the condition of Al/Si = 1, half of the zeolites' Si atoms were chosen randomly, and replaced with Al's atoms.
2- The Na⁺ ions were randomly located in the zeolite structure.
3- According to the following stopping criteria, an energy minimization was done to put Na⁺ cations in their minimum energy state in the zeolite structures.
The iterations were terminated when one of the stopping criteria was satisfied (the stopping tolerance for energy (unitless), stopping tolerance for force (Kcal/mol.Angstrom), the maximum iterations of minimizer, and the maximum number of force/energy evaluations were set to 10^{-25}, 10^{-25}, 500000, and 1000000 respectively).
4- For complete constructing of the simulation boxes, the reformed zeolite structures were put in the middle of the box. Also, the heavy-metal and Cl⁻ Ions were located in two sides of the structure randomly.
5- In order to put the heavy-metal and Cl⁻ Ions in their minimum states, another energy minimization with same stopping criteria was performed.
The detailed descriptions of simulation boxes are summarized in Table 2. The ratio of positive charge of all metal ions over Na⁺ ions in the structure was set equal to unity. Since, the number of heavy-metal ions was half of the number of Cl⁻ and Na⁺, the divalent heavy-metal ions were used in all simulations.

Table 1.
LJ parameters, atomic charges and ionic radii of atoms and ions.

Atoms/ions	σ (Å)	ε (kJ/mol)	q (e)	Ionic radius (Å) [29]
Si	3.914	0.263	+1.540	0.410
Al	3.936	0.019	+1.110	0.500
O	2.760	0.426	-0.9125	1.400
Na⁺	2.584	0.099	+1.000	0.950
Pb²⁺	3.829	0.662	+2.000	1.200
Cd²⁺	2.537	0.228	+2.000	0.970
Cu²⁺	3.114	0.005	+2.000	0.690
Cl⁻	4.400	0.100	-1.000	1.810

Table 2.
Simulation boxes characteristics.

Zeolite	Unit cell chemical formula [30]	a (Å)	b (Å)	c (Å)
LTJ	$Al_8Si_8O_{32}$	55.50	27.75	30.24
ANA	$AL_{24}Si_{24}O_{96}$	82.38	27.46	27.46
SVR	$Al_{92}Si_{92}O_{384}$	122.48	26.60	42.32
MER	$Al_{16}Si_{16}O_{64}$	84.69	28.46	39.78
AFY	$Al_8Si_8O_{32}$	50.99	25.5	36.06
BEC	$Al_{16}Si_{16}O_{64}$	76.62	25.54	26
MEL	$AL_{48}Si_{48}O_{192}$	120.40	40.14	26.82
SGT	$Al_{32}Si_{32}O_{128}$	61.43	30.72	34.38
SAO	$Al_{28}Si_{28}O_{112}$	80.63	26.88	43.72
OBW	$Al_{38}Si_{38}O_{152}$	83.48	27.82	30.84
SBT	$Al_{72}Si_{72}O_{288}$	103.14	34.40	41.03
FAU	$Al_{96}Si_{96}O_{384}$	150.16	25.03	25.03
VFI	$Al_{18}Si_{18}O_{72}$	113.85	37.95	32.42
TSC	$Al_{192}Si_{192}O_{768}$	122.96	30.74	30.74

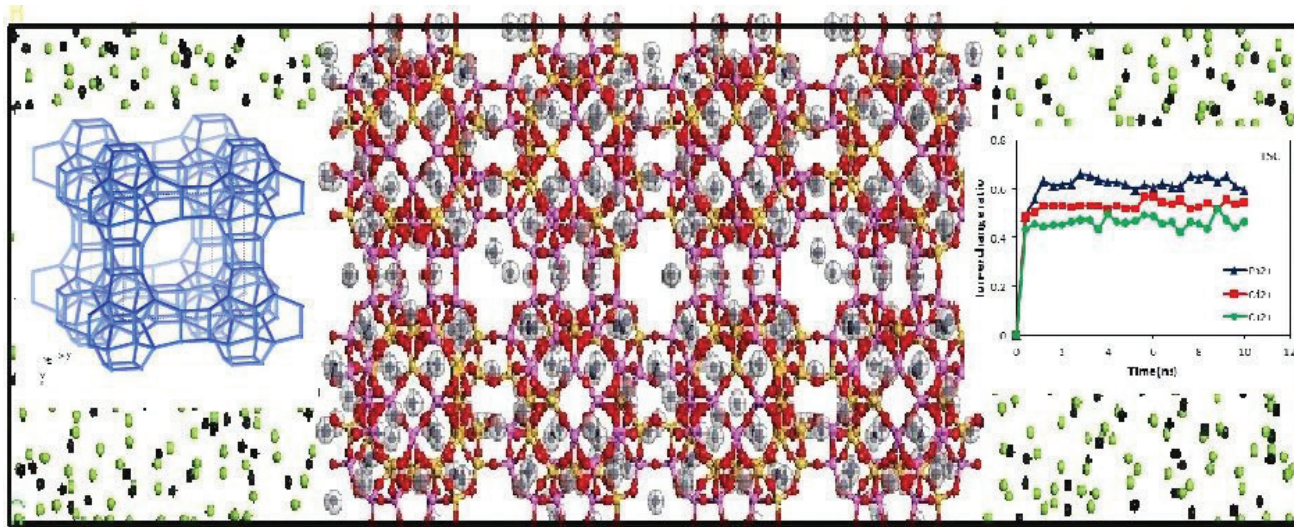(a, b, c) simulation box lengths in respectively x, y, z directions.

Fig. 1. The schematic of the simulation box for TSC zeolite structure and Cu^{2+} and Cl^- ions in two sides of the structure; Si: yellow; O: red; Al: pink; Cu^2+: black balls; Cl^-: green balls; Na^+: purple balls with a plus sign.

Fig. 1, schematically shows a simulation box for TSC zeolite and Cu^{2+} and Cl^- ions in two sides of the zeolite structural model. In this simulation box, there are 384 Na^+, 384 Al, 384 Si, 1522 O, 384 Cl^-, and 192 Cu^{2+} ions.

The pore size of zeolites are described with parameters such as the maximum diameter of a sphere (D_i) and maximum diameter of a sphere (D_d) that can diffuse along [30]. All zeolites have the same D_i in all three directions, but different D_d parameter in various directions. Two groups of zeolites were chosen to perform molecular dynamics simulations. The first group (includes the LTJ, ANA, SVR, BEC, MEL, SGT, SAO, FAU and TSC) had the equal D_d parameter in three directions. This zeolites is named as symmetric type zeolites and are summarized in Table 3 [30]. The second group (includes the MER, AFY, OBW, SBT and VFI) have the same D_d parameter in a direction and b direction but different in the c direction [30]. Therefore, they are named the asymmetric zeolites and are summarized in Table 4.

The framework flexibility was neglected and except for Na^+ ions, other zeolite atoms (including Al, Si and O) were held fixed. The periodic boundary condition was used in all directions, and simulations were performed at constant 300 K with Noose–Hoover thermostat [28]. The MD simulations were done with time step of 1 fs for 10 ns, including two parts: the first 2 ns was the equilibration part, and the second 8 ns was the production part. Each 5ps, the coordinates of all ions were saved to analyze the results.

Table 3.
Symmetric zeolites with the same D_d in all three directions [30].

Zeolites	D_i (Å)	D_d (Å)
LTJ	4.1	3.12
ANA	4.21	2.43
SVR	5.85	4.65
BEC	6.95	6.09
MEL	7.72	5.19
SGT	7.74	2.11
SAO	8.64	6.79
FAU	11.24	7.35
TSC	16.45	4.08

The MD simulations were done at 300 K in a system consisting only single ions of Cd (II), Cu (II) and Pb (II) in symmetric type zeolites and asymmetric type zeolites. The mean IERs were evaluated according to their D parameters to investigate the effect of zeolite pore size (D_d and D_i in symmetric and D_d (a,b), D_d(c) and D_i in asymmetric zeolites).

The triple-ion systems with an equal amount of three ions were simulated for the LTJ, ANA, SVR, BEC, MER zeolites to survey the competitive condition. In addition, the temperature effect was explored in the temperature range of 300-345 K for the systems containing Copper (II) for the LTJ, ANA, SVR, BEC, MER zeolites.

Table 4.
Asymmetric zeolites with different Dd in c direction [30]

Zeolites	D_i (Å)	D_d (Å) a, b direction	D_d (Å) c direction
MER	6.65	3.12	4.20
AFY	7.82	4.08	5.90
OBW	9.26	5.18	3.62
SBT	11.17	7.34	5.71
VFI	12.03	2.4	11.39

3. Results and discussion

3.1. Single-ion system

In the systems containing one metal ion, the process dynamics were analyzed by calculating of the IER. This ratio was the number of exchanged Na^+ ions to the number of initial Na^+ ions in the zeolite structure. Fig. 2 shows the Na^+ IERs versus simulation time in the ANA, AFY, OBW, FAU, and TSC zeolites. The ratio time averages for all the one-ion systems are summarized in Table 5. In this table, zeolite structural models, including SVR, BEC, MEL, SGT, SAO, OBW, SBT, FAU, VFI, and TSC has the highest affinity for exchanging ion with Lead (II) and the lowest affinity for Copper (II). This results well agreed with experimental reports [4,7 and 8]. This phenomenon can be explained by the larger ionic size of the Lead (II) ions. Since, they are in closer distance from the zeolite wall atoms and consequently, have higher interactions with the zeolite wall atoms.
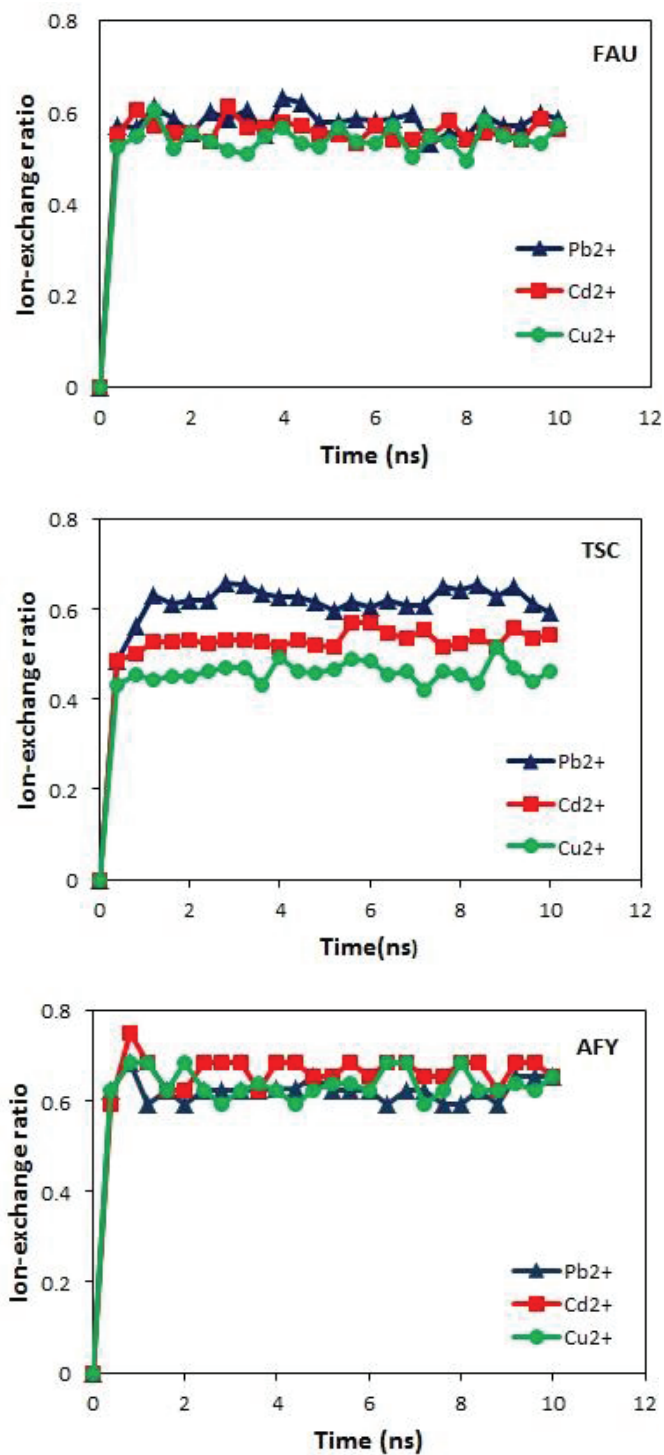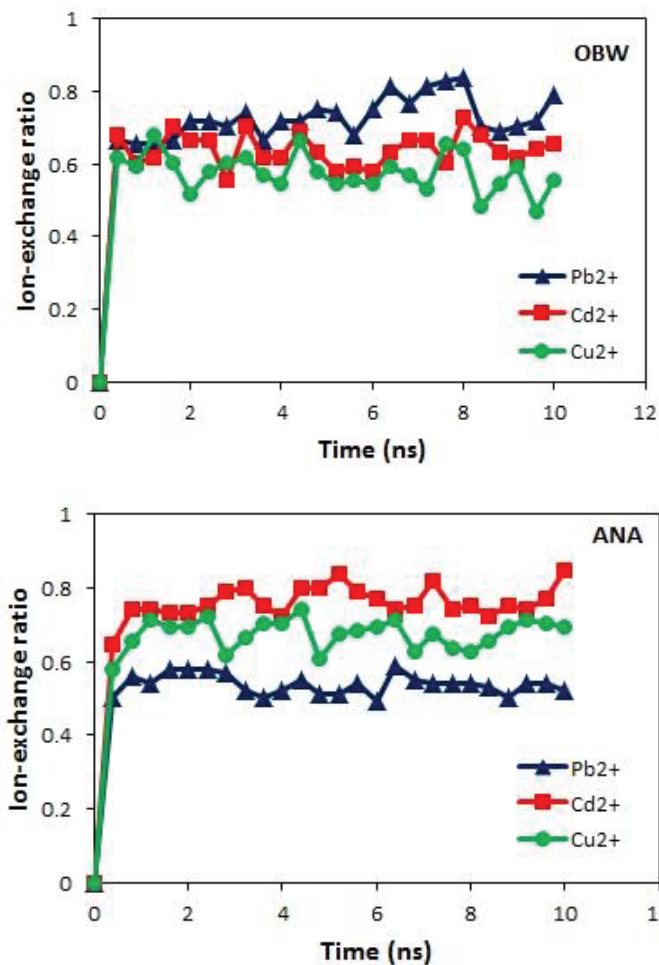

Fig. 2. Ion-exchange ratio versus simulation time for the systems containing each ion of Pb^{2+}, Cd^{2+}, and Cu^{2+} for the ANA, OBW, AFY, FAU, and TSC zeolites.

Table 5.
The mean ion-exchange ratio (MIER) in one-ion systems

Zeolites	Ion	MIER	Zeolites	Ion	MIER
	Pb^{2+}	0.54		Pb^{2+}	0.60
ANA	Cd^{2+}	0.76	SGT	Cd^{2+}	0.52
	Cu^{2+}	0.67		Cu^{2+}	0.48
	Pb^{2+}	0.74		Pb^{2+}	0.72
SVR	Cd^{2+}	0.62	SAO	Cd^{2+}	0.61
	Cu^{2+}	0.56		Cu^{2+}	0.55
	Pb^{2+}	0.58		Pb^{2+}	0.72
LTJ	Cd^{2+}	0.72	OBW	Cd^{2+}	0.64
	Cu^{2+}	0.63		Cu^{2+}	0.58
	Pb^{2+}	0.57		Pb^{2+}	0.68
MER	Cd^{2+}	0.69	SBT	Cd^{2+}	0.63
	Cu^{2+}	0.62		Cu^{2+}	0.59
	Pb^{2+}	0.63		Pb^{2+}	0.58
AFY	Cd^{2+}	0.69	FAU	Cd^{2+}	0.56
	Cu^{2+}	0.65		Cu^{2+}	0.54
	Pb^{2+}	0.75		Pb^{2+}	0.48
BEC	Cd^{2+}	0.61	VFI	Cd^{2+}	0.47
	Cu^{2+}	0.52		Cu^{2+}	0.45
	Pb^{2+}	0.69		Pb^{2+}	0.62
MEL	Cd^{2+}	0.58	TSC	Cd^{2+}	0.53
	Cu^{2+}	0.50		Cu^{2+}	0.46

For further analyses, radial distribution function (RDF) was also calculated in support of the obtained results. The RDFs of the pairs (Al, Cd^{2+}), (Al, Cu^{2+}), and (Al, Pb^{2+}) in the one-ion systems for the ANA, OBW, AFY, FAU, and TSC zeolites was shown in Fig. 3. The RDF results show that for each zeolite, the ion with the largest mean IER gives the highest peak. Also, the ion with the lowest IER gives the shortest peak. This phenomenon verifies the obtained results from IERs. This means that except for ANA, LTJ, MER and AFY zeolite structures which the highest peaks in RDF diagrams belong to Cd^{2+} ions, the highest peaks belong to Pb^{2+} ions.
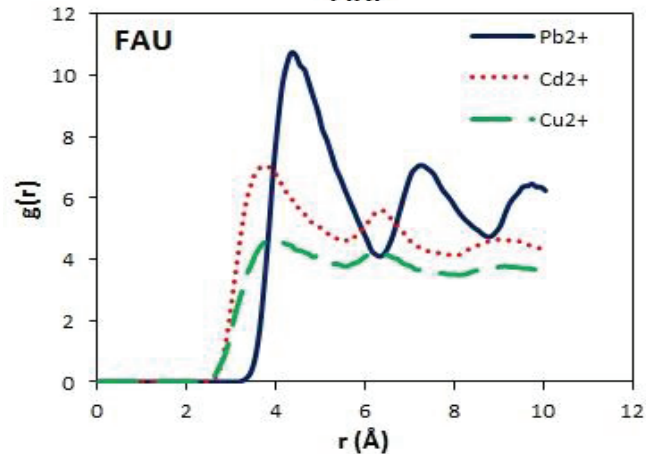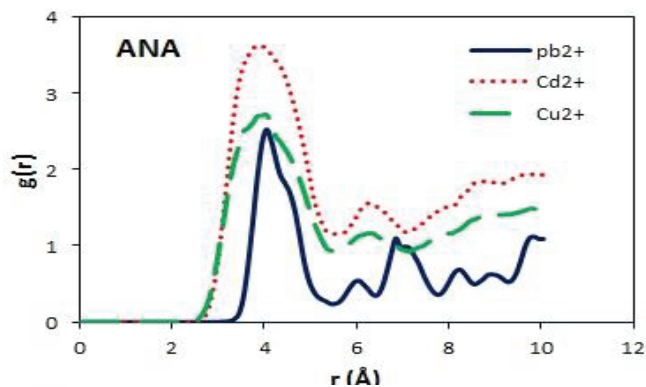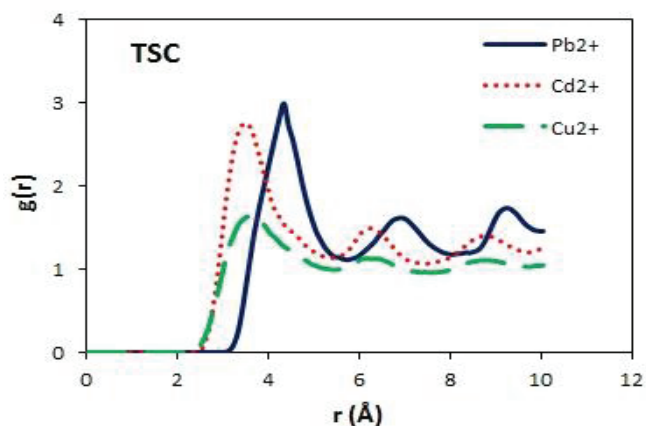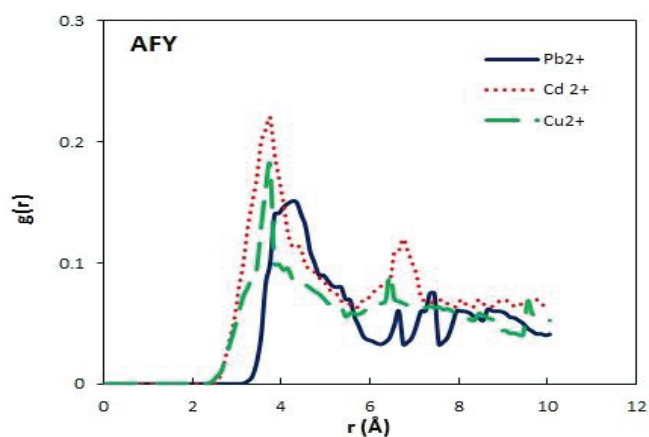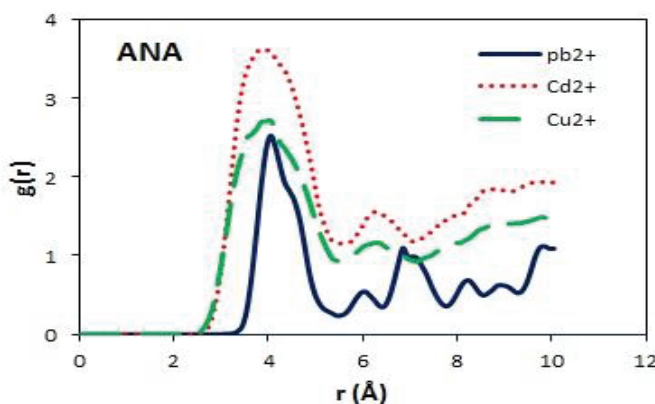

Fig. 3. The RDFs of the pairs Al–Pb^{2+}, Al–Cd^{2+}, and Al–Cu^{2+} in the systems containing each of the ions for the ANA, OBW, AFY, FAU, and TSC zeolites.

3.2. Multi- ion systems

Triple-ion systems with equal amounts of Cd^{2+}, Cu^{2+}, and Pb^{2+} ions were simulated at 300 K. Results are summarized in Table 6. The zeolites which had the maximum mean IERs for Cd^{2+} and Cu^{2+} (LTJ, ANA, SVR, BEC and MEL) were chosen to perform the simulations. The BEC and SVR zeolites had the maximum mean IERs for Pb^{2+} ion. Here, the IER for each ion is defined as a number of exchanged heavy-metal ions to their initial numbers in the solution.

Table 6.
The mean ion-exchange ratio (MIER) in single and multi-ion

Zeolite	Ion	MIER in one-ion systems	MIER in multi-ion systems
ANA	Cd^{2+}	0.76	0.73
	Cu^{2+}	0.67	0.39
	Pb^{2+}	0.54	0.34
BEC	Cd^{2+}	0.61	0.60
	Cu^{2+}	0.52	0.23
	Pb^{2+}	0.75	0.94
LTJ	Cd^{2+}	0.72	0.71
	Cu^{2+}	0.63	0.39
	Pb^{2+}	0.58	0.54
MEL	Cd^{2+}	0.58	0.36
	Cu^{2+}	0.50	0.15
	Pb^{2+}	0.69	0.94
SVR	Cd^{2+}	0.62	0.49
	Cu^{2+}	0.56	0.15
	Pb^{2+}	0.74	0.84

As in Table 6, the affinity for single ion system in the zeolites of BEC, MEL, and SVR was in the order of $Pb^{2+}> Cd^{2+}> Cu^{2+}$. Moreover, this order remains in the competitive condition of ion mixture. However, in ANA and LTJ zeolites, because of smaller Di parameters, which are comparable to Pb^{2+} ionic size, the affinity order becomes: $Cd^{2+}> Cu^{2+}> Pb^{2+}$. This is in the same as competitive condition that does not change the affinity of zeolites for the ions. This agrees the results of Nalaparaju et al. [4].

3.3. Pore size effect

The calculated mean ion-exchange ratios (MIER) of the studied zeolites are reported in Table 5. The MIERs for the symmetric zeolites versus their D_i and D_d parameters are plotted in Fig. 4 and 5.
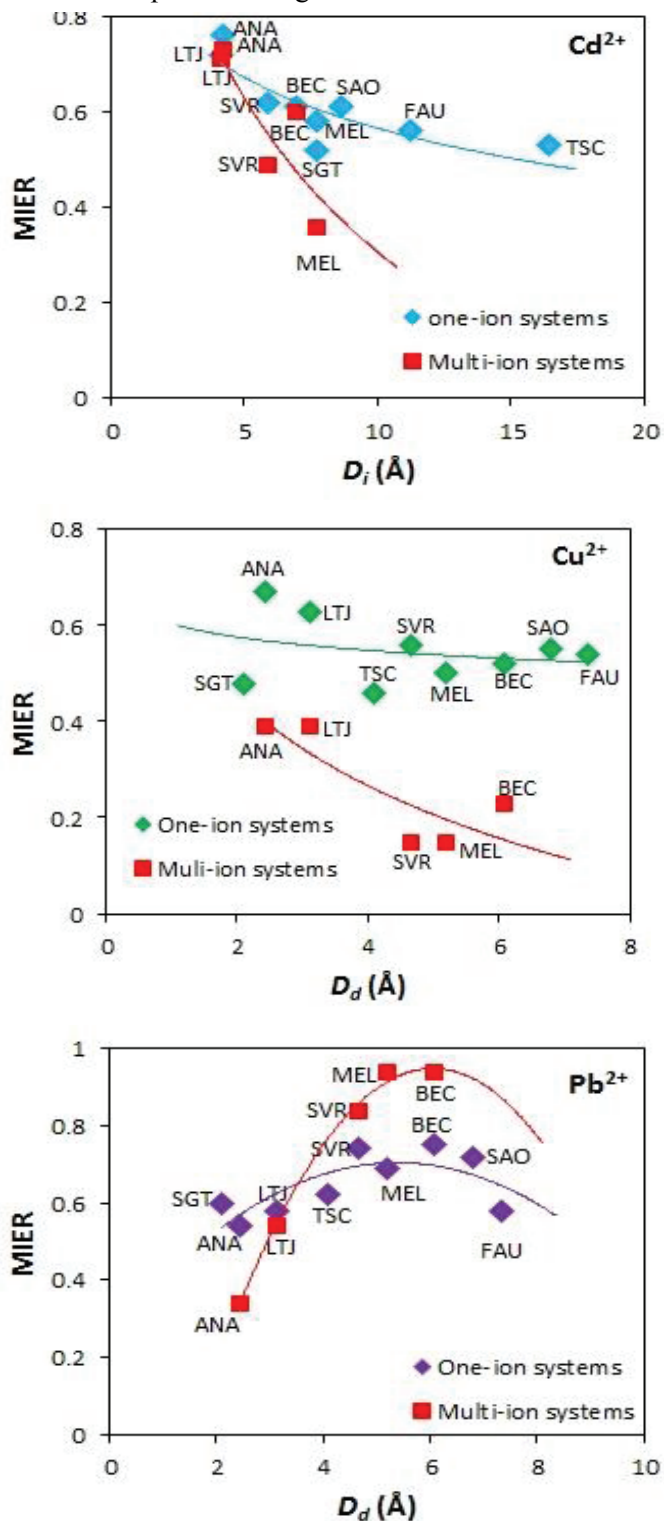

Fig. 4. The mean ion-exchange ratio (MIER) in symmetric zeolites versus their Dd parameters (The continuous lines show the trend).
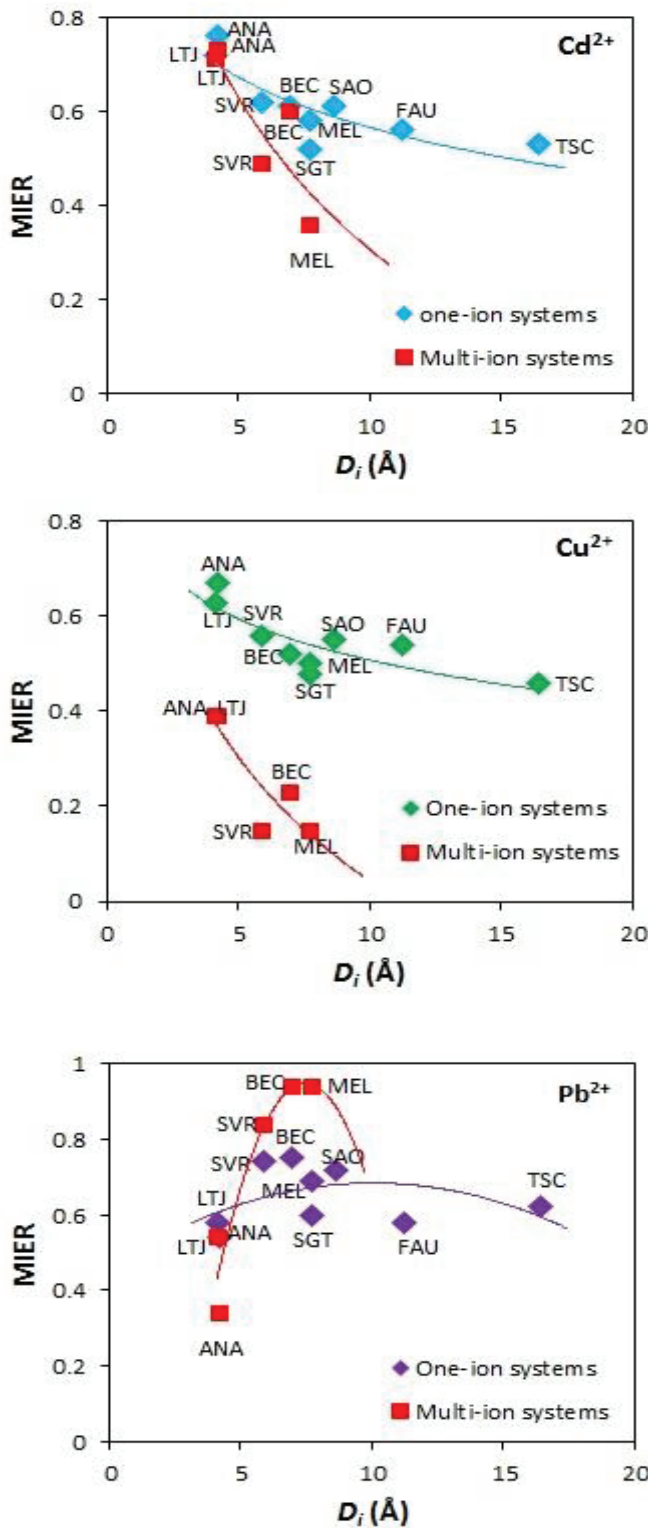
Fig. 5. The mean ion-exchange ratio (MIER) in symmetric zeolites versus their Di parameters (The continuous lines show the trend).

D_i, is the diameter of the largest possible sphere which can be included. D_d, is the diameter of the largest free sphere that can diffuse through the framework of zeolite structure at least by one lattice dimension [30]. As shown in from Figures 4, 5 and Table 5, Cd^{2+} and Cu^{2+} have the highest MIERs in zeolites of ANA and LTJ when they contact with a single-ion system. Furthermore, the same behavior is observed in a mixture with other two ions.

The results also indicate that in the zeolites with larger Di and Dd parameters, MIER was reduced. This can be explained by considering that, in the zeolites with large pores and free spaces (ionic diameters of Cu^{2+} and Cd^{2+} are respectively 0.69 and 0.97 Å), the most of the ions are present in the bulk of electrolyte. Hence, they are far away from the zeolite wall and cannot interact properly with the wall atoms. Consequently, the attraction forces which pull the metal ions to come into contact the ion-exchanging sites would be less effective.

As shown in Figure 3, the first peak(is the most intense one) represent the most probable distance for presence of electrolyte ions near to the Al atoms in the zeolite framework. It appears approximately at a distance less ~4 Å which nearly corresponds to the average Lennard–Jones (LJ) size parameter (Equation 2):

$$\sigma_{ij} = \frac{\sigma_i + \sigma_j}{2} \tag{2}$$

Where σ_i and σ_j are the (LJ) parameters of the ion in the electrolyte and the atom in the zeolite framework.

As shown in Figures 4 and 5, the same decreasing behavior of MIER is seen in the zeolites with larger Di and Dd in the ion electrolyte mixtures for the ions of Cu^{2+} and Cd^{2+}. The lower MIER of the ions in the mixture compared with those of one ion systems indicates the presence of competition for ion exchanging and occupation of ion exchanging sites by other ions in the mixture.

Figures 4 and 5 show a different behavior of Cu^{2+} and Cd^{2+} in Pb^{2+} ion exchange with the zeolites. That is, for D_i and D_d parameters up to the 6 Å, there is a rise in MIER values and then decrease, both for only Pb^{2+} and for Pb^{2+} in the mixture. The ionic radius of Pb^{2+} (1.+Å) is very higher than those of Cu^{2+} and Cd^{2+}. The average LJ calculated size parameters for Pb^{2+} and Al pair and Pb^{2+} and Si pair is 3.882 Å and 3.871 Å, respectively. Also, as given in Table 7, calculated ε for the ion pair Pb^{2+} and Al is 0.112 kJ/mol.

Table 7.
The average Lennard-Jones (LJ) size parameters.

Ions	Zeolites atoms	σ_{ave} (Å)
Pb^{2+}	Al	3.882
	Si	3.871
	O	3.294
Cd^{2+}	Al	3.236
	Si	3.225
	O	2.648
Cu^{2+}	Al	3.525
	Si	3.514
	O	2.937

Therefore, for zeolite with D_i and D_d parameters up to 6 Å, the Pb^{2+} ions would occupy the available ion-exchange sites in the aperture of the pores. This is due to larger ionic size and high attraction to sites in the zeolites' pore walls. Consequently, it impedes further penetration of Pb^{2+} ions into the pores BEC and SVR zeolites which have the optimum pore sizes and the highest MIER values. This is explained by the fact that, the pores are not so small to block the penetration of ions due to attraction to the pore aperture. Also, not so wide that and thereby, the attraction forces become ineffective.

As it is seen from Fig. 4 and 5, for the Lead (II) ions in the mixture, the MIERs are higher than those for the systems containing only single Lead (II) ions. This observation can be attributed to the increase in the ionic strength of the ions in the mixture. Consequently, this phenomenon increases the repulsion forces between the positive ions Cd^{2+}, Cu^{2+} and Pb^{2+}. This reason pushes the ions from the bulk to the zeolites' pores walls and since Pb^{2+} has higher affinity for attraction due to higher LJ energy parameters. Therefore, it occupies more ion-exchange sites in the zeolites pores compared with the systems containing only Pb^{2+} ions.

The reason for decrease of MIER in the mixture is competitive ion exchange with the zeolites as well as the higher affinity of Pb^{2+} for absorption through the zeolite wall. Consequently, it increases the site occupation by Pb^{2+} and decreases the available ion-exchange sites for Cu^{2+} and Cd^{2+}. Therefore, this effect appears as a decrease in the MIER values for Cu^{2+} and Cd^{2+} in the ion mixtures. The asymmetric zeolites are those which are anisotropic in three free space directions available for the diffusion. That is, they have pores with different D_d values for x, y and z directions. As shown in Figure 6, the MIERs variations indicate an increase and then a decrease in D_d and D_i. For example, OBW and AFY zeolite, which are shown in Figure 3, it is expected that the most probable distance of heavy-metal ions from Al's atoms in the zeolite's structures is approximately between 2–4 Å. Therefore, zeolites with D_d parameters less than 4 Å have experienced a retardation in their movement and restriction in occupying the sites. Also, zeolites with larger D parameters, the ions are less affected by the attraction forces imposed by the zeolite walls.

In Fig. 6, MIER for Pb^{2+} is higher than those for Cu^{2+} and Cd^{2+}. This can be attributed to the higher ε parameter of Pb^{2+} compared with the other two ions. Also, the increasing of MIER to a maximum value and then its decrement can be attributed to presence of pores with different sizes in three dimensions, which facilitate the attraction of ions to zeolites' pore walls. But, as the pore size passes the optimum value for AFY and OBW zeolites, as expected the MIER begins to descend. Hence, AFY and OBW have the highest affinity to ion exchange with heavy-metal ions of Cd^{2+}, Cu^{2+} and Pb^{2+}.

3.4. Temperature effect

To temperature effect investigation, the molecular dynamics simulations were done at the 300, 315, 330, and 345 K for only Copper (II) ion system. The LTJ, ANA, SVR, BEC and MER zeolites were used for the simulations. The temperature coefficients of MIER, defined as (d[MIER])/dt, were calculated for a number of zeolites and are presented in Table 8. The results indicate a very small temperature coefficient. Therefore, the effect of temperature variation on MIER is insignificant. This is in agreement with both experimental and simulation studies [6,26].
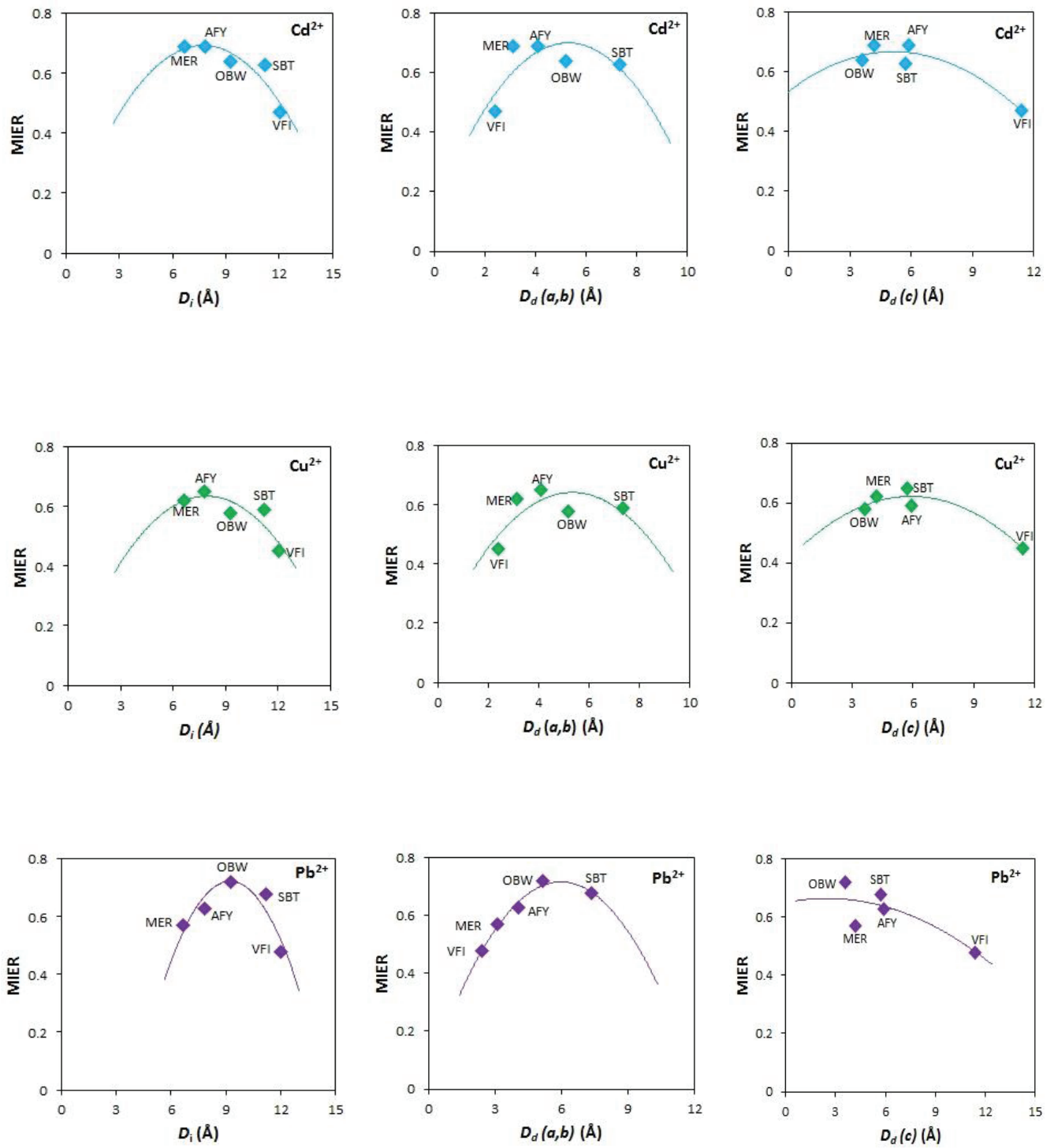
Fig. 6. The mean ion-exchange ratio (MIER) in asymmetric zeolites versus their Di, Dd(a,b) and Dd(c) parameters for one-ion systems (The continuous lines show the trend).

Table 8.
The temperature effect on the mean ion-exchange ratio (MIER)

Zeolites	Temperature (K)	MIER	$\frac{d[MIER]}{dT}$ (K^{-1})
ANA	300.00	0.67	
	315.00	0.68	$+ 0.66 \times 10^{-4}$
	330.00	0.68	0
	345.00	0.69	$+ 0.66 \times 10^{-4}$
LTJ	300.00	0.62	
	315.00	0.64	$+ 1.32 \times 10^{-4}$
	330.00	0.66	$+ 1.32 \times 10^{-4}$
	345.00	0.65	$- 0.66 \times 10^{-4}$
SVR	300.00	0.56	
	315.00	0.57	$+ 0.66 \times 10^{-4}$
	330.00	0.59	$+ 1.32 \times 10^{-4}$
	345.00	0.58	$- 0.66 \times 10^{-4}$
BEC	300.00	0.52	
	315.00	0.51	$- 0.66 \times 10^{-4}$
	330.00	0.52	$+ 0.66 \times 10^{-4}$
	345.00	0.51	$- 0.66 \times 10^{-4}$
MEL	300.00	0.51	
	315.00	0.51	0
	330.00	0.52	$+ 0.66 \times 10^{-4}$
	345.00	0.51	$- 0.66 \times 10^{-4}$

4. Conclusions

The ion-exchange of heavy metal ions Cu^{2+}, Cd^{2+} and Pb^{2+} with the number of symmetric and asymmetric zeolites with various structural models and varied pore size were investigated by molecular dynamics simulation. The results indicated that the MIERs of zeolites for these ions depend on various parameters such as pore size, their free space for the diffusion, diameter of ion, Lennard–Jones size and energy parameters. The same trend was followed in the ion-exchange affinity of zeolites for each ion in a single electrolyte and in mixtures. The results indicated that, for ion-exchanging with Pb^{2+}, the affinity of zeolites was higher than other two heavy-metal ions. The calculated temperature coefficient for the MIERs indicated no significant changes on temperature variation.

References

[1] M. E. Argun, Use of clinoptilolite for the removal of nickel ions from water: Kinetics and thermodynamics, J. Hazard. Mater. 150 (2008) 587-595.

[2] M. Sprynskyy, B. Buszewski, A. P. Terzyk, J. Namieśnik, Study of the selection mechanism of heavy metal (Pb^{2+}, $Cu^{2+,}$ Ni^{2+}, and Cd^{2+}) adsorption on clinoptilolite, J. Colloid Interface Sci. 304 (2006) 21-28.

[3] R. Petrus, J. K. Warchoł, Heavy metal removal by clinoptilolite. An equilibrium study in multi-component systems, Water Res. 39 (2005) 819-830.

[4] A. Nalaparaju, Z. Q. Hu, X. S. Zhao, J. W. Jiang, Exchange of heavy metal ions in titanosilicate Na-ETS-10 membrane from molecular dynamics simulations, J. Membrane Sci. 335 (2009) 89-95.

[5] F. Pepe, B. de Gennaro, P. Aprea, D. Caputo, Natural zeolites for heavy metals removal from aqueous solutions: Modeling of the fixed bed Ba^{2+}/Na^{+} ion-exchange process using a mixed phillipsite/chabazite-rich tuff, Chem. Eng. J. 219 (2013) 37-42.

[6] A. A. Ismail, R. M. Mohamed, I. A. Ibrahim, G. Kini, B. Koopman, Synthesis, optimization and characterization of zeolite A and its ion-exchange properties, Colloids Surf. A 366 (2010) 80-87.

[7] S. Ahmed, S. Chughtai, M.A. Keane, The removal of cadmium and lead from aqueous solution by ion exchange with Na-Y zeolite, Sep. Purif. Technol. 13 (1998) 57-64.

[8] K. D. Mondale, R. M. Carland, F. F. Aplan, The comparative ion exchange capacities of natural sedimentary and synthetic zeolite, Miner. Eng. 8 (1995) 535-548.

[9] S. K. Pitcher, R. C. T. Slade, N. I. Ward, Heavy metal removal from motorway stormwater using zeolites, Sci. Total. Environ. 334–335 (2004) 161-166.

[10] T. S. Jamil, H. S. Ibrahim, I. H. Abd El-Maksoud, S. T. El-Wakeel, Application of zeolite prepared from Egyptian kaolin for removal of heavy metals: I. Optimum conditions, Desalination 258 (2010) 34-40.

[11] B. Biškup, B. Subotić, Kinetic analysis of the exchange processes between sodium ions from zeolite A and cadmium, copper and nickel ions from solutions, Sep. Purif. Technol. 37 (2004) 17-31.

[12] K. S. Hui, C. Y. H. Chao, S. C. Kot, Removal of mixed heavy metal ions in wastewater by zeolite 4A and residual products from recycled coal fly ash, J. Hazard. Mater. 127 (2005) 89-101.

[13] H. Mekatel, S. Amokrane, A. Benturki, D. Nibou, Treatment of Polluted Aqueous Solutions by Ni^{2+}, Pb^{2+}, Zn^{2+}, Cr^{+6}, Cd^{+2} and Co^{+2} Ions by Ion Exchange Process Using Faujasite Zeolite, Procedia Eng. 33 (2012) 52-57.

[14] R. Navarrete-Casas, A. Navarrete-Guijosa, C. Valenzuela-Calahorro, J. D. López-González, A. García-Rodríguez, Study of lithium ion exchange by two synthetic zeolites: Kinetics and equilibrium, J. Colloid Interface Sci. 306 (2007) 345-353.

[15] G. Onyestyák, Solid-state ion exchange dynamics of cadmium in zeolite Y, Stud. Surf. Sci. Catal. 174 (2008) 877-880.

[16] J. Hou, J. Yuan, R. Shang, Synthesis and characterization of zeolite W and its ion-exchange properties to K^+ in seawater, Powder Technol. 226 (2012) 222-224.

[17] L. Ćurković, Š. Cerjan-Stefanović, T. Filipan, Metal ion exchange by natural and modified zeolites, Water Res. 31 (1997) 1379-1382.

[18] A. H. Ören, A. Kaya, Factors affecting adsorption characteristics of Zn (II) on two natural zeolites, J. Hazard. Mater. 131 (2006) 59-65.

[19] P. Fletcher, R. P. Townsend, Ion-exchange of amminated palladium and platinum in synthetic sodium zeolites, Zeolites 3 (1983) 129-133.

[20] P. Demontis, G. B. Suffritti, A comment on the flexibility of framework in molecular dynamics simulations of zeolites, Micropor. Mesopor. Mater. 125 (2009) 160-168.

[21] L. Benco, T. Demuth, J. Hafner, F. Hutschka, Ab initio molecular dynamics simulation of hydration and ion-exchange processes in low Al-zeolites, Micropor. Mesopor. Mater. 42 (2001) 1-19.

[22] C. F. Mellot, A. K. Cheetham, Monte Carlo simulations of extraframework cation positions in dehydrated zeolite LiX (Si:Al = 1.25), C. R. Acad. Sci. IIC - Chem. 1 (1998) 737-744.

[23] V. V. Guliants, J. T. Mullhaupt, J. M. Newsam, A. M. Gorman, C. M. Freeman, Predicting locations of non-framework species in zeolite materials, Catal. Today 50 (1999) 661-668.

[24] J. Lignières, J. M. Newsam, Simulations of the non-framework cation configurations in dehydrated Na–Ca and Na–Li zeolite A, Micropor. Mesopor. Mater. 28 (1999) 305-314.

[25] A. Miyamoto, M. Kubo, Structure and Dynamics of Ion-exchanged Zeolites as Investigated by Molecular Dynamics and Computer Graphics, Stud. Surf. Sci. Catal. 83 (1994) 117-124.

[26] R. Ekhteiari Salmas, B. Demir, E. Yıldırım, A. Sirkecioğlu, M. Yurtsever, M. G. Ahunbay, Silver−Sodium Ion Exchange Dynamics in LTA Zeolite Membranes, J. Phys. Chem. C. 117 (2013) 1663-1671.

[27] M. P. Allen, D. J. Tildesley, Computer Simulation of Liquids, Clarendon Press, Oxford, U.K., 1988.

[28] K. M. Ralls, T. H. Courtney, J. Wulff, Introduction to Materials Science and Engineering, John Wiley & Sons, New York, 1976.

[29] http://www.iza-structure.org/databases.

[30] M. D. Foster, I. Rivin, M. M. J. Treacy, O. Delgado Friedrichs, A geometric solution to the largest-free-sphere problem in zeolite frameworks, Micropor. Mesopor. Mater. 90 (2006) 32-38.